Development of New Sustainable Inorganic Flame Retardant Additive System for Polyamide 6,6 With Improved Performance

Imane Belyamani,[1] Joshua U. Otaigbe,[1] William R. Fielding[2]
[1] *School of Polymers and High Performance Materials, The University of Southern Mississippi, Hattiesburg, Mississippi 39406*
[2] *Great Lakes Solutions, Chemtura Corporation, West Lafayette, Indiana 47906*

We report the effect of new sustainable inorganic phosphate glass (P-glass) flame retardants for polyamide 6,6 (PA6,6). Three P-glasses differing in chemical composition and glass transition temperature (T_g) were prepared and their flame retardant effect on PA6,6 was studied by cone calorimetry, thermogravimetric analysis, and SEM-EDX. The effect of high and intermediate T_g P-glasses on the thermal stability of PA6,6 was negligible as compared to that of the low T_g P-glass due to the hygroscopic nature of the latter. However, the char formation was independent of the P-glass composition and was observed to increase by 30% in the presence of P-glass. The low T_g P-glass composition (i.e., ILT-1) was found to be a promising flame retardant for PA6,6 at a concentration of up to 15% by weight. Cone calorimetry data showed that the ILT-1 decreased both the peak heat release rate and the total heat amount released from the PA6,6/ILT-1 hybrids, resulting in an efficient formation of a glassy char layer. In contrast to the intermediate and high T_g P-glasses of this study, SEM-EDX indicated that the ILT-1 P-glass was well dispersed in the PA6,6 matrix to yield a typical droplet-in-matrix phase morphology in the melt-blended binary immiscible P-glass/PA6,6 hybrids. POLYM. ENG. SCI., 55:1741–1748, 2015. © 2014 Society of Plastics Engineers

INTRODUCTION

Engineered polyamides are used widely in electronic or electrical equipment, military and civil infrastructure applications because of their excellent mechanical properties, heat resistance, oil resistance [1, 2], and thermal stability [3]. Flame retardancy (FR) of polyamides used in electrical and electronic equipment has been a topical challenge for a long time. Effective solutions have included halogen-based flame retardant additives. Commercially available flame retardants cannot satisfy all applications and expectations. For example, the global consumption of flame retardant chemicals is estimated at 4 billion lbs. for 2013, and is expected to reach 5.2 billion lbs. in 2018, a 5-year compound annual growth rate of 5% for the period 2013 to 2018 [4]. Therefore, development of new advanced halogen-free flame retarded systems has spurred research and development interests in the last few years [5–18].

A number of reported studies in the literature have shown that phosphorous compounds can act in both the condensed and the gaseous phases, resulting in highly efficient flame retardant properties. For example, Czegeny and Blazso [6] have reported that during gradual heating of polymer/ammonium phosphate and polymer/phosphoric acid mixtures, the char formation is significantly increased. Their results were explained by the formation of intumescent foam layer on the surface by the gaseous products evolved from polymers. The hindered diffusion of these products into the gas phase facilitates crosslinking, leading to char formation. More recently, Saucă et al. [12] have demonstrated that a chemically modified poly(vinyl alcohol) with a phosphorous-containing reagent can lead to high charred barrier formation in the condensed phase. In addition, the authors just mentioned reported that flame resistance in the gas phase is possible because volatile phosphate derivatives were identified in the volatile mixture after the degradation process. Further, other researchers have reported synergistic effects between several additives based on phosphorous compounds to enhance the flame retardant properties of polymers [8, 9, 11, 18–20]. For example, in a recent study carried out by Xu et al. [11], a synergistic effect between PTPA (poly[N^4-bis(ethylenediamino)-phenyl phosphonic-N^2, N^6-bis(ethylenediamino)-1,3,5-triazine-*N*-phenyl phosphonate]) and ammonium polyphosphate (APP) has been demonstrated, resulting in high flame retardant efficiency indicated by a limited oxygen index of 32% and a V-0 rating in UL-94. In addition, Laachachi et al. [19] have reported synergistic effects between alumina nanoparticles and APP-based additives, leading to an improvement of PMMA fire behavior performance indicated by high ignition times, reduced heat release rate (HRR), reduced total heat released, and significant increase of total burning time.

Recently, the use of inorganic compounds containing phosphorous to improve flame retardant properties of polymers has increased significantly, thus providing a complement to existing halogenated substances [21]. Among the phosphorous-based compounds, inorganic phosphate glasses (P-glasses) display a wide range of desirable properties such as chemical durability, high thermal expansion, good electrical conductivity, optical clarity, biocompatibility [22], and flame retardant properties [23–25]. P-glasses are polymeric in nature as they are composed of chain-like or crosslinked structures that are very similar to polymer chain networks [26]. Very few studies have focused on the flame retardant properties of P-glass in organic polymers. Ferrarini and Feltzin [25] reported that the fire retardance of a resin containing moisture-resistant low melting P-glass was improved by the liberation of nonflammable gases after thermal decomposition. More recently, Siebecker et al. [23] have discovered a flame retardant additive system comprising low glass transition temperature (T_g) P-glass, phosphinic acid salt, zinc salt, and melamine salt, and have reported that it has a combination of improved physical and flame resistance properties.

Correspondence to: Joshua U. Otaigbe; e-mail: Joshua.Otaigbe@usm.edu
Contract grant sponsor: Great Lakes Solutions, Chemtura Corporation.
DOI 10.1002/pen.24012
Published online in Wiley Online Library (wileyonlinelibrary.com).

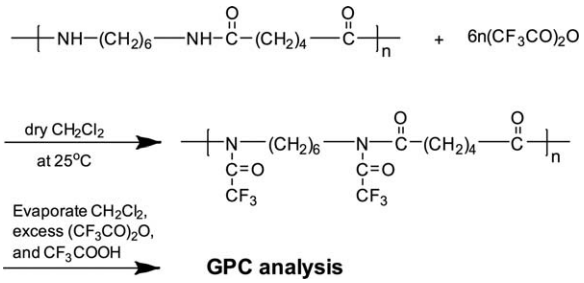

FIG. 1. Modification of PA6,6 via trifluoroacetylation in order to make it soluble in THF for GPC analysis.

The objective of this work described in this article is to study the effect of special new P-glass compositions with varying glass transition temperatures on the processing conditions of polyamide 6,6 (PA6,6) and the final hybrid structure and FR. The mechanism of the FR behavior of the P-glasses in PA6,6 is described and the FR property will be shown to be strongly dependent on the type of the reactants used to prepare inorganic phosphate glass compositions.

MATERIALS AND METHODS

Materials

PA6,6 (Dupon't Zytel® 101) was used in the experiments described in the following sections. It was dried in a vacuum oven maintained at 80 ± 1°C and a vacuum pressure of 700 mm Hg until a water content of 0.1% was achieved. The water content was measured using a moisture analyzer (OHAUS, MB35, Parsippany, NJ) at 160°C for 45 min.

A comprehensive literature review revealed a number of patents illustrating the preparation of inorganic glasses based on inorganic phosphates with different T_g values. The T_g values are related to the type and the stoichiometric molar concentrations of the reactants used. In this study, P-glass compositions with three different glass transition temperatures were synthesized in the laboratory according to procedures reported elsewhere by Otaigbe and Beall [26], Tick [27], Beall and Quinn [28], and Beall and Pierson [29]. The tin fluorophosphate glass composition (hereinafter denoted as ILT-1) gave a T_g of approximately 104°C. The mixed alkali zinc phosphate glasses with an intermediate T_g (hereinafter denoted as IIT-3) and a high T_g (hereinafter denoted as IHT-1) gave respectively glass transition temperatures of ~192°C and ~314°C.

Melt Processing, Compounding and Characterization Methods

Internal Batch Mixing. Melt processing operations were carried out on the dry PA6,6, using a thermo-Haake Polydrive® batch mixer at a temperature of 263°C (Zones 1, 2, and 3). Firstly, the polymer was added to the mixing bowl (at time, $t = 0$) and allowed to mix for 2.5 min in order to yield a homogeneous melt. The P-glass was subsequently introduced into the mixer in the required amounts (i.e., 2, 8, and 15 wt%) and allowed to mix for an additional 2.5 min. The rotor speed was fixed at 75 rpm.

Compression Molding. Cone calorimeter samples were prepared by compression molding the PA6,6/P-glass hybrids and the pure PA6,6 into 6.5 × 6.5 × 3 mm square plaques following standard methods. The compression molding conditions were set as follows: Temperature = 269°C, Pressure = 100 MPa, and mold residence time = 4.45 min

Thermogravimetric Analysis. Thermal stability of PA6,6/P-glass hybrids was investigated under inert atmosphere using a Thermal Analysis Q500 instrument Thermogravimetric Analyzer. Nitrogen was used as purging gas. Tests were performed from 30 to 600°C at a heating rate of 10°C/min.

Fire Properties via Cone Calorimetry. Combustion behavior was evaluated in a Govmark® CC-1 cone calorimeter following standard procedures [30]. The bottom and the sides of each specimen, prepared by compression molding, were wrapped in an aluminum foil and exposed horizontally to an irradiation at 35 kW/m^2 and data were collected during the entire combustion time. The heat released was calculated from the consumption of oxygen due to combustion. The HRR (kW/m^2) and its peak value (PHRR, kW/m^2) were automatically obtained from the computer software. The reported values represent the average of two replicates. The dimensions of the specimens used were 6.5 × 6.5 × 3 mm.

Scanning Electron Microscopy/Energy-Dispersive X-ray Spectroscopy. A high-resolution scanning electron microscopy (SEM) equipped with energy dispersive X-ray (EDX) was used to characterize the morphology of the PA6,6/P-glass hybrids. The SEM investigation and EDX analysis were obtained from cryofractured surface of the samples. The cross-sectional sample was prepared by cryogenic fracture in liquid nitrogen and then sputter-coated with gold for 3 min, to provide a conductive 10 nm thickness of gold coating prior to the SEM/EDX measurements.

Trifluoroacetylation of PA6,6 and Gel Permeation Chromatography. To use gel-permeation Chromatography (GPC), PA6,6 was modified via trifluoroacetylation as depicted in Fig. 1, according to previously reported procedure by Weisskopf and Meyerhoff [31]. Approximately 50 mg of PA6,6 was added to a

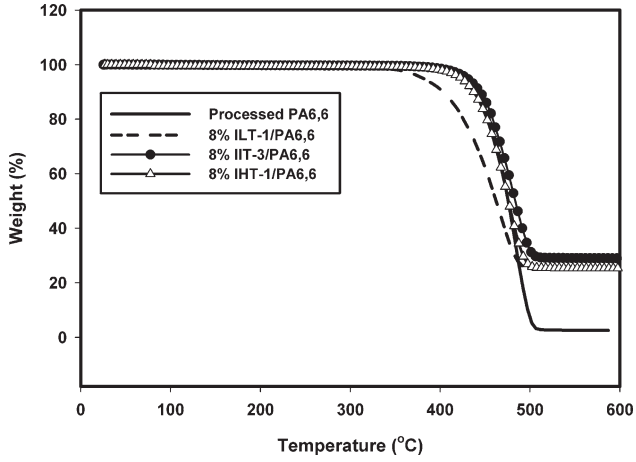

FIG. 2. Thermogravimetric analysis (TGA) data obtained from pure PA6,6 and PA6,6/8% P-glass hybrids.

DOI 10.1002/pen

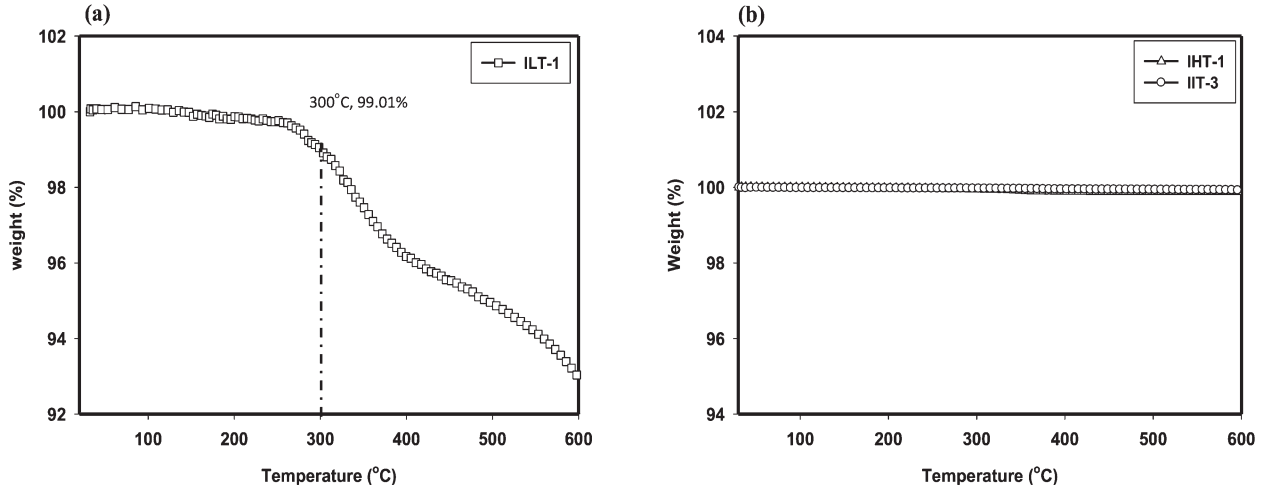

FIG. 3. TGA data obtained from: (a) ILT-1, (b) IIT-3, and IHT-1.

flask capped with a rubber septum, and the flask was flushed with N_2 using a hypodermic needle for 10 min. Subsequently, 1.5 ml dry methylene chloride (CH_2Cl_2) was added to the flask followed by the addition of a threefold molar excess of trifluoroacetic anhydride (TFAA). The reaction was allowed to run overnight at room temperature after which the TFAA modified

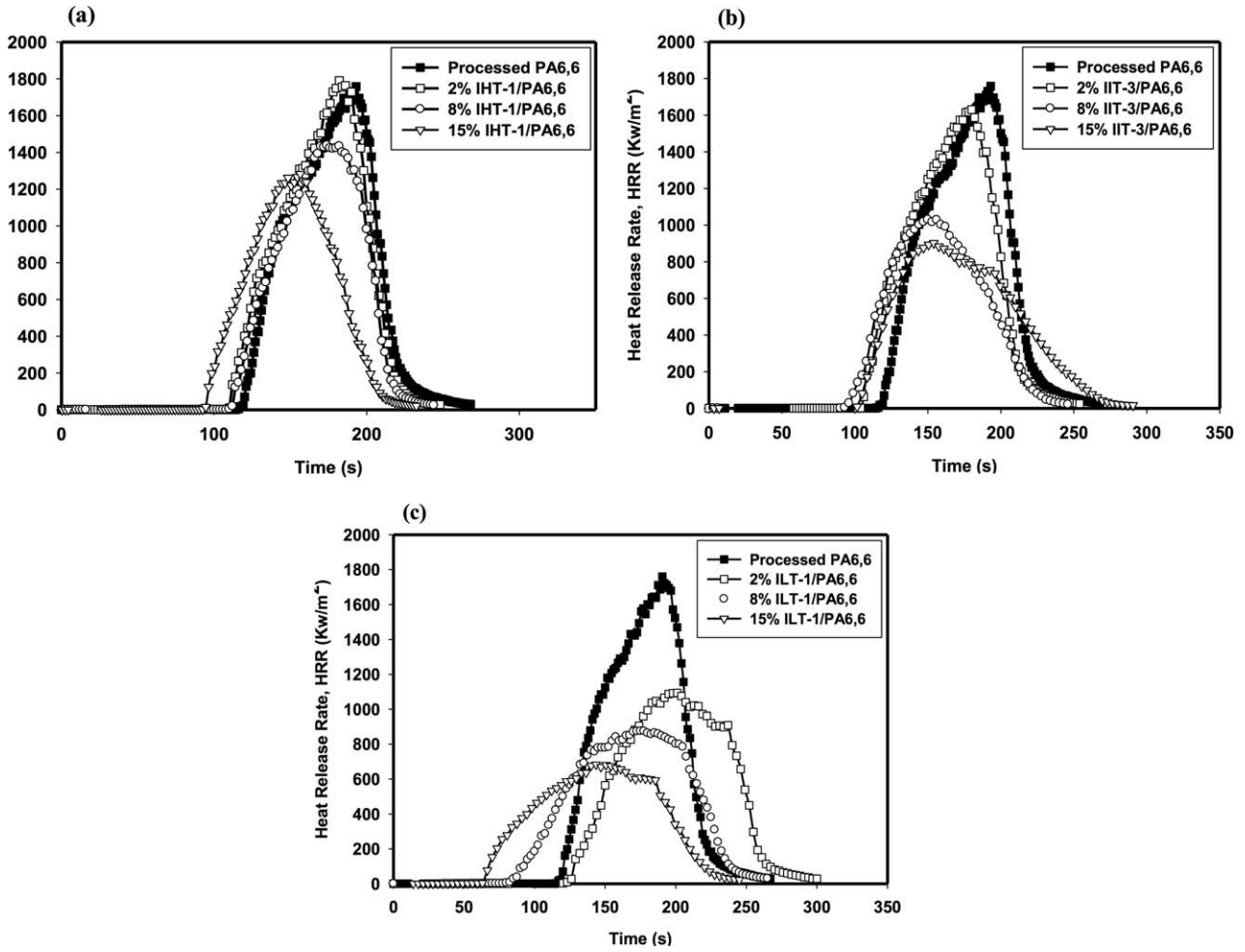

FIG. 4. Comparison of the HRR plots for (a) PA6,6/IHT-1; (b) PA6,6/IIT-3; and (c) PA6,6/ILT-1 hybrids, at different mass fractions of P-glass indicated, at 35 kW/m ^{2} heat flux.

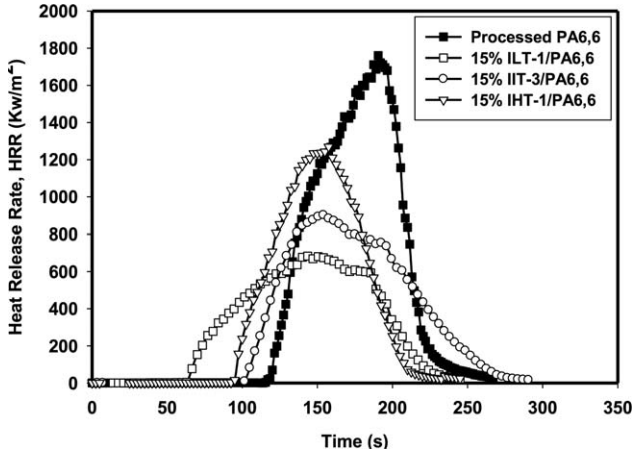

FIG. 5. Comparison of the HRR plots for PA6,6 compounded with 15% IHT-1, 15% IIT−3 and 15% ILT-1, at 35 kW/m ^{2} heat flux

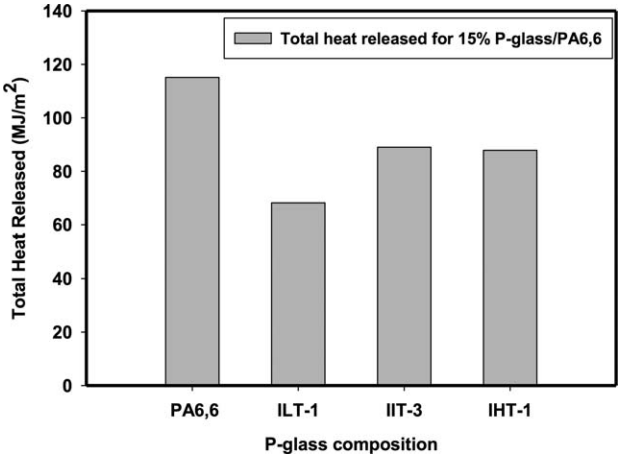

FIG. 7. Comparison of the total heat released by 15% P-glass/PA6,6 hybrids as a function of P-glass type at 35 kW/m ^{2} heat flux.

PA6,6 (TFAA-PA6,6) was isolated by evaporating CH_2Cl_2, excess TFAA, and trifluoroacetic acid (TFA). 1 ml dry CH_2Cl_2 was then added again to dissolve the isolated TFAA-PA6,6. Adding CH_2Cl_2 helped to dissolve TFAA-PA6,6 in dry THF to prepare the GPC samples with a concentration of 5 mg/ml.

RESULTS AND DISCUSSION

Thermal Stability of PA6,6/P-Glass Hybrids

Figure 2 shows the percent weight loss of pure PA6,6 and PA6,6/P-glass hybrids as a function of temperature prepared as already described in the previous section. It is clearly evident in this figure that the pure PA6,6, and PA6,6/8% IIT-3 and PA6,6/8% IHT-1 hybrids showed thermal degradation beginning at ~400°C which corresponds to the thermal degradation of pure PA6,6. For PA6,6/8% ILT-1 hybrid, the thermal degradation occurs earlier (between 300 and 350°C) as Fig. 2 shows. As expected, the first evidence of weight loss is ascribed to the absorbed water evaporation of the hybrid which is consistent with the hygroscopic nature of the ILT-1 P-glass compared to that of IIT-3 and IHT-1 P-glasses which are relatively nonhygroscopic and thermally stable (see Fig. 3). Additionally, the earlier weight loss of PA6,6/ILT-1 hybrid may also be due to the chemical interaction between PA6,6 and ILT-1.

Further, at 500°C PA6,6 is almost completely degraded with a $\leq$ 5 wt% residue (Fig. 2). In contrast, 25 to 30 wt% of PA6,6/P-glass hybrids residues were obtained and found to be relatively thermally stable at 500°C, confirming our expectation of improved performance of P-glass as a char forming flame retardant in PA6,6.

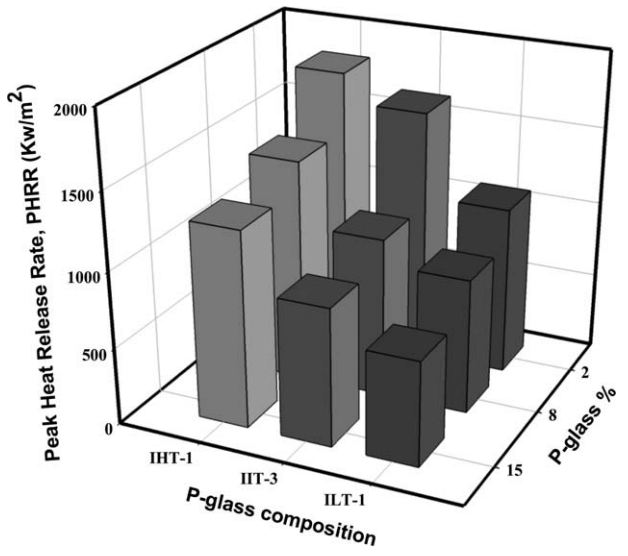

FIG. 6. Comparison of the peak HRR (PHRR) plots for PA6,6/P-glass hybrids, as a function of the P-glass composition and concentration at 35 kW/m^2 heat flux.

Fire Properties of PA6,6/P-Glass Hybrids

As already described a cone calorimeter was used in this study to accurately measure fire-relevant properties such as HRR and carbon monoxide yield among other fire related properties. The HRR plots for PA6,6/P-glass samples, at different concentrations of P-glass, as compared to that of the pure PA6,6, are shown in Fig. 4.

The cone calorimetry data shows reduced HRRs for PA6,6/P-glass samples. This reduction is more significant when PA6,6 was compounded, even at low loading, with the low T_g P-glass (ILT-1). In contrast, the IIT-3 and IHT-1 showed a decreasing effect on the HRR of the hybrid materials, only when added to PA6,6 at relatively high P-glass mass fractions (8, 15 wt%). Figure 4 also shows different types of typical burning behavior which are summarized in Fig. 5 for easy comparison.

Clearly, from both Figs. 4 and 5 and according to Schartel and Hull [32] the following features are discernable: (1) The HRR curve shape of PA6,6/IHT−1 hybrids is similar to that of pure PA6,6, and shows a sharp HRR peak regardless of the P-glass concentration, implying that the whole sample is completely pyrolysed; (2) For PA6,6/IIT-3, a similar behavior is observed at low P-glass concentration (2 and 8 wt%) but at 15% of P-glass the fire behavior of the material showed an initial increase in HRR and as the char layer thickens the HRR

 DOI 10.1002/pen

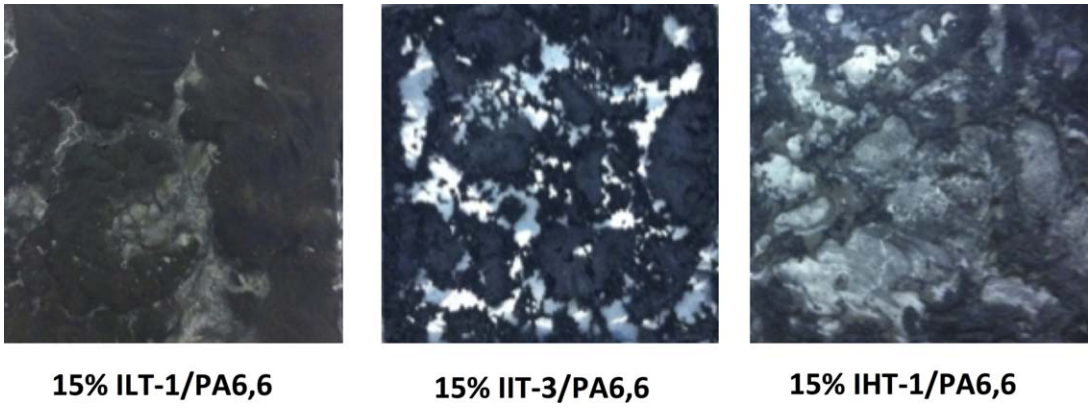

FIG. 8. Pictures of the char residues taken after total sample combustion. [Color figure can be viewed in the online issue, which is available at wileyonlinelibrary.com.]

decreased progressively, implying that the formed char layer is not very efficient or is cracked; and (3) When PA6,6 was compounded with low T_g P-glass (i.e., ILT-1), the HRR curves showed different fire behavior, depending on the P-glass concentration, that are all related to the formation of a multi-layer char. However, this phenomenon just mentioned is more pronounced for PA6,6/15% ILT-1 as evidenced by the presence of a large peak that is consistent with the formation of a thick and efficient char layer.

Plotting the samples' peak HRR (PHRR) was found to be the most important parameter to evaluate fire safety as it is related to the char layer formation [33]. Moreover, the representation of the total heat released by each sample should reveal the efficiency of the formed char layer. Figures 6 and 7, respectively, depict the samples PHRR versus P-glass composition and concentration curves and the total heat quantity released by PA6,6/15% P-glass hybrids as a function of P-glass type. It is clear from Fig. 6 that the PHRR values decrease with increasing P-glass concentration regardless of their composition. Additionally, PHRR of PA6,6/ILT-1 samples showed a significant reduction as compared to that of PA6,6/IIT-3 and PA6,6/IHT-1 samples. The PHRR data also indicate that the samples containing 15% ILT-1 seem to be more efficient in forming a char layer. These results are consistent with the total heat quantity released by PA6,6/15% P-glass hybrids shown in Fig. 7. The PA6,6/15% ILT-1 released less heat during the combustion as compared to that of the other hybrids and the neat polymer. This is believed to be due to the formation of an efficient glassy layer that leads to a decrease in the heat and mass transfer.

The experimental findings of this study are consistent with the following mechanisms that have been proposed by Gilman et al. [34] and Zhu et al. [35] to explain how nanocomposite formation can reduce the PHRR of a polymer: (1) The degradation of PA6,6/P-glass samples during the combustion produces a multilayered carbonaceous-phosphorous structure that may act as an excellent insulator and also as a barrier to mass transport; and (2) The presence of phosphorous in P-glass can lead to some radical trapping reactions that will lower the HRR. In addition, a comparison of the residue char pictures (taken after total combustion in the Cone Calorimeter) for the each of the samples (Fig. 8) was found to be in agreement with the PHRR and the total heat amount released data already discussed. Clearly, Fig. 8 shows the formation of an efficient char layer for samples containing ILT-1 and a cracked char layer in the samples containing IHT-1 and IIT-3, suggesting

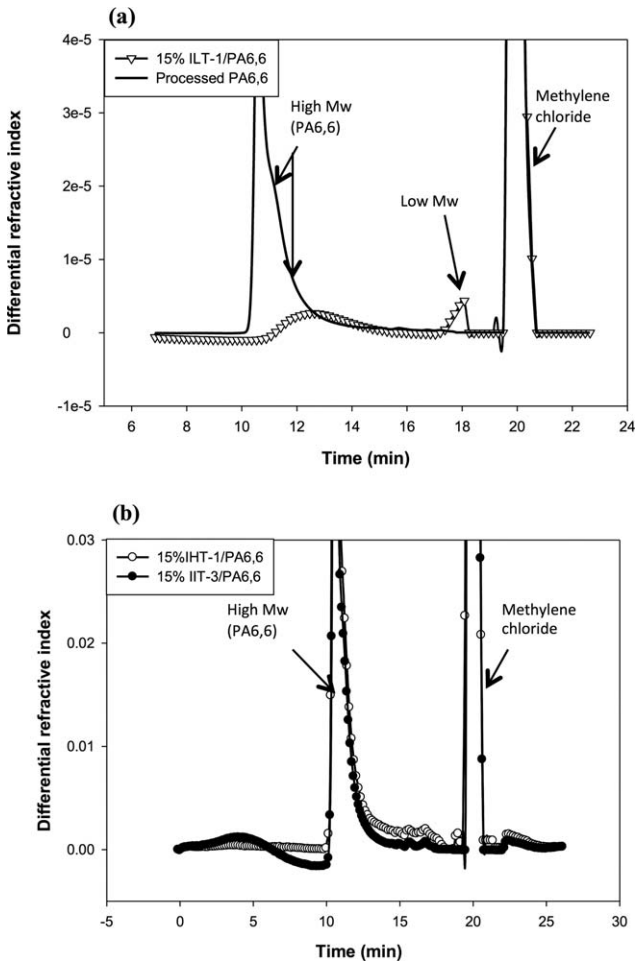

FIG. 9. GPC traces obtained from: (a) 15% ILT-1/PA6,6 hybrids and pure processed PA6,6 and (b) PA6,6/15% IIT-3 and PA6,6/15% IHT-1 hybrids.

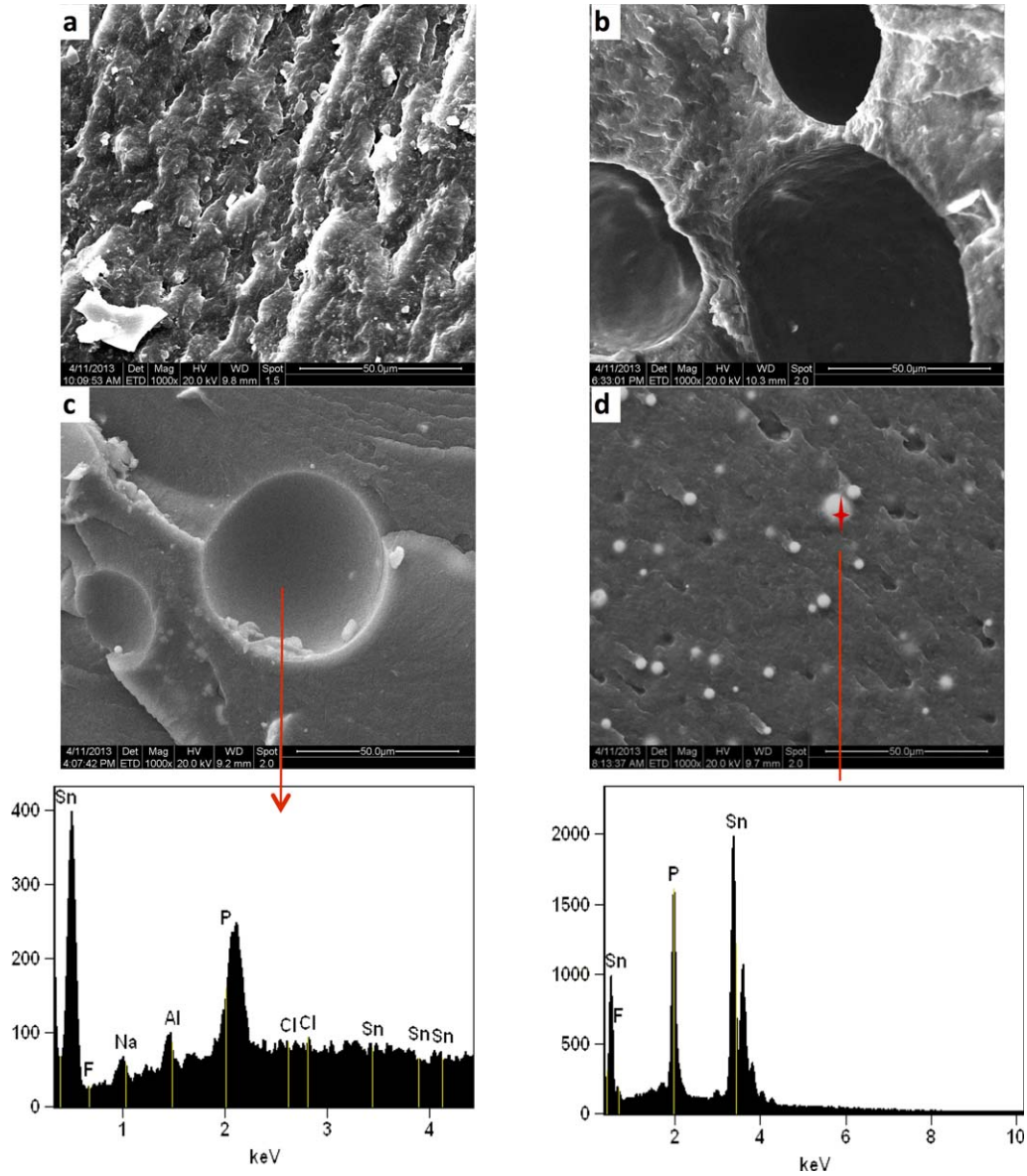

FIG. 10. Representative SEM micrographs for cryofractured surface of: (a) processed virgin PA6,6; (b) PA6,6/8% IIT-3; (c) PA6,6/8% IHT-1; and (d) PA6,6/8% ILT-1 hybrids with EDX analysis of the red spots. [Color figure can be viewed in the online issue, which is available at wileyonlinelibrary.com.]

that ILT-1 is particularly efficient as a char forming flame retardant in PA6,6. The addition of ILT-1 to PA6,6 results in decreased PHRR and total amount of heat released from the PA6,6/ILT-1 hybrids through the formation of an efficient glassy char layer. In fact, as was reported by Jahromi et al. [5], during the combustion process, the phosphate is transformed into phosphoric acid by thermal degradation. The phosphoric acid formed is known to act simultaneously as a degrading agent and a crosslinker of the thermal degradation products of PA6,6.

GPC analysis of the PA6,6/P-glass hybrids was found to be a reliable method for evaluating the eventual chemical interaction between P-glass and PA6,6 in the hybrids. Figure 9 shows the GPC traces from PA6,6/15% P-glass hybrids as compared to that of the melt processed virgin PA6,6. It is clearly evident in Fig. 9 that a peak corresponding to low molecular weight (M_w) fractions appears only when PA6,6 is blended with 15% ILT-1 as compared to melt processed virgin PA6,6. The GPC curves confirmed that a chemical interaction between P-glass and PA6,6 occurred, leading to chain scission of the polyamide. It is worthy to note that this interaction facilitates the thermal degradation of PA6,6. However, this is not the case for the PA6,6/IHT-1 and PA6,6/IIT-3 hybrid samples because no low molecular peak was observed in the corresponding GPC curves as Fig. 9b shows.

The general mechanism of phosphorous fire retardant action is reported elsewhere for APP/PA6 blends [36–38] to be according the following chemical reaction:

 DOI 10.1002/pen

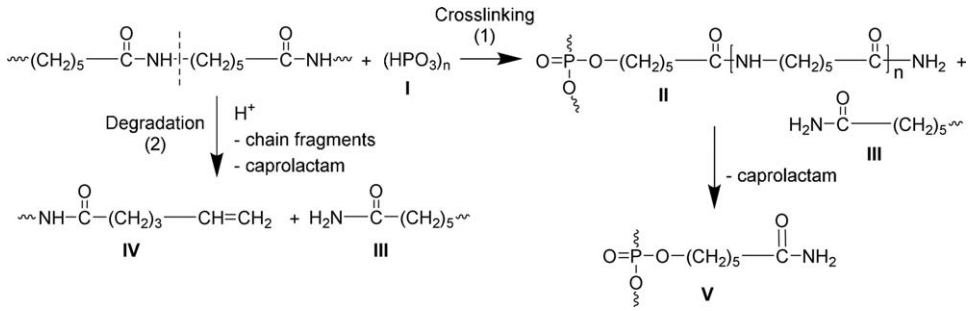

The amidopentyl polyphosphate (II) formed in reaction (1) decomposes on further heating in an inert atmosphere, producing a high temperature phosphorus oxynitride-type solid residue (V). Both the aliphatic-aromatic (II) and phosphorus oxynitride (V) residues can act as reinforcing material for the intumescent protective char made from the foamed viscous polyphosphoric acid on the surface of burning composite. The obtained crosslinking residues act as a barrier which is expected to prevent oxygen and heat from reaching the substrate thereby blocking the transfer of flammable materials into the gas phase.

From the preceding experimental results and discussion, it can be concluded that mixing the low T_g P-glass (ILT-1) with PA6,6 facilitates hydrolytic chain scission of the PA6,6 macromolecules via a chemical interaction between the phosphate and the alpha-Carbon of the amide bonds of PA6,6.

Morphology of PA6,6/P-Glass Hybrids Studied by SEM/EDX

Figure 10 shows representative scanning electron micrographs of the cryofractured surface of processed PA6,6, PA6,6/8% ILT-1, PA6,6/8% IHT-1, and PA6,6/8% IIT-3 hybrids and the energy dispersive X-ray spectroscopy (EDX) analysis of the red spots. The SEM micrographs show a typical droplet-in-matrix phase morphology in the melt-blended binary immiscible hybrids of this study.

The size and the shape of the dispersed phase were found to vary as a function of the P-glass composition and T_g. In addition, the SEM images show that ILT-1 is well dispersed in the PA6,6 matrix, in contrast to intermediate and high T_g P-glass/PA6,6 hybrids. Further, the EDX analysis of the dispersed droplets gave reasonably accurate quantitative amounts of all the original elements of the respective P-glass compositions used to prepare the tested P-glass/PA6,6 hybrid compounds, namely, F, Sn, and P for low T_g P-glass and P, Sn, Al, Na, and Cl for high T_g P-glass.

CONCLUSIONS

The effect of using different flame retardant system additives based on inorganic phosphorous on the FR properties of PA6,6 was investigated. The results show that mixing low T_g P-glass with PA6,6 facilitates hydrolytic chain scission of the PA6,6 macromolecules through chemical interaction between phosphate and the alpha-Carbon of the amide bonds of the PA6,6, leading to better flame retardant properties. Only 15 wt% of ILT-1 in PA6,6 decreased the PHRR and the total amount of heat released from the PA6,6/ILT-1 hybrids studied through formation of an efficient glassy char layer. These experimental facts were found to be consistent with the results from SEM-EDX analysis which showed a good dispersion of ILT-1 in the PA6,6 matrix compared to the other P-glass compositions with intermediate and high glass transition temperatures. This study may spur further studies in academia and industry aimed at assessing the impact of incorporating P-glass flame retardants on other key properties of organic polymers such as mechanical performance, viscoelastic behavior, long-term durability along with aesthetic properties and cost-effectiveness so that ready-to-use products with market acceptance could be designed.

ACKNOWLEDGMENTS

The technical assistance of Drs. Sergei Nazarenko and Charles Manzi-Nshuti in acquisition and analysis of the cone calorimetery data and Dr. Andreas Plagge in carrying out the SEM-EDX analysis is gratefully acknowledged. Garrett Campbell and Dr. Robson Storey are also acknowledged for their help with the GPC analysis.

REFERENCES

1. T. Moriwaki, *Compos. Part Appl. Sci. Manuf.*, **27**, 379 (1996).
2. M.K. Akkapeddi, *Polym. Compos.*, **21**, 576 (2000).
3. A. Bernasconi, P. Davoli, D. Rossin, and C. Armanni, *Compos. Part Appl. Sci. Manuf.*, **38**, 710 (2007).
4. Anonymous, "Market Research reports and Technical Publications: Product Catalog," *BCC Research*, Wellesley, MA (www.bccresearch.com), March (2014).
5. S. Jahromi, W. Gabriëlse, and A. Braam, *Polymer*, **44**, 25 (2003).
6. Z. Czégény and M. Blazsó, *J. Anal. Appl. Pyrolysis*, **81**, 218 (2008).
7. G. Tang, X. Wang, R. Zhang, W. Yang, Y. Hu, L. Song, and X. Gong, *Compos. Part A: Appl. Sci. Manuf.*, **54**, 1 (2013).
8. A. Laachachi, M. Cochez, E. Leroy, M. Ferriol, and J.M. Lopez-Cuesta, *Polym. Degrad. Stab.*, **92**, 61 (2007).
9. U. Braun, B. Schartel, M.A. Fichera, and C. Jäger, *Polym. Degrad. Stab.*, **92**, 1528 (2007).
10. W. Jou, K. Chen, D. Chao, C. Lin, and J. Yeh, *Polym. Degrad. Stab.*, **74**, 239 (2001).
11. Z.-Z. Xu, J.-Q. Huang, M.-J. Chen, Y. Tan, and Y.-Z. Wang, *Polym. Degrad. Stab.*, **98**, 2011 (2013).
12. S. Saucă, M. Giamberini, and J.A. Reina, *Polym. Degrad. Stab.*, **98**, 453 (2013).

13. E. Gallo, U. Braun, B. Schartel, P. Russo, and D. Acierno, *Polym. Degrad. Stab.*, **94**, 1245 (2009).
14. Q. Tai, R.K.K. Yuen, W. Yang, Z. Qiao, L. Song, and Y. Hu, *Compos. Part Appl. Sci. Manuf.*, **43**, 415 (2012).
15. D. Enescu, A. Frache, M. Lavaselli, O. Monticelli, and F. Marino, *Polym. Degrad. Stab.*, **98**, 297 (2013).
16. Y. Chen and Q. Wang, *Polym. Degrad. Stab.*, **91**, 2003 (2006).
17. P. Kiliaris, C.D. Papaspyrides, R. Xalter, and R. Pfaendner, *Polym. Degrad. Stab.*, **97**, 1215 (2012).
18. F. Samyn and S. Bourbigot, *Polym. Degrad. Stab.*, **97**, 2217 (2012).
19. A. Laachachi, M. Cochez, E. Leroy, P. Gaudon, M. Ferriol, and J.M. Lopez Cuesta, *Polym. Adv. Technol.*, **17**, 327 (2006).
20. S. Bourbigot, S. Duquesne, G. Fontaine, S. Bellayer, T. Turf, and F. Samyn, *Mol. Cryst. Liq. Cryst.*, **486**, 325/[1367] (2008).
21. D. Purser, "Chapter 24 Influence of Fire Retardants on Toxic and Environmental Hazards from Fires," in *Fire Retardancy of Polymers: New Strategies and Mechanisms*, T.R. Hull and B.K. Kandola, Eds., RSC Publishing, Cambridge, UK, 381 (2009).
22. C.-K. Loong, K. Suzuya, D.L. Price, B.C. Sales, and L.A. Boatner, *Phys. B Condens. Matter*, **241–243**, 890 (1997).
23. J. Siebecker, W. Fielding, and J. Otaigbe, U.S. Patent 02867511 (2011).
24. J.U. Otaigbe, C.J. Quinn, and G.H. Beall, *Polym. Compos.*, **19**, 18 (1998).
25. L.J. Ferrarini Jr. and J. Feltzin, U.S. Patent 4,079,022 (1978).
26. J.U. Otaigbe and G.H. Beall, *Trends Polym. Sci.*, **5**, 369 (1997).
27. P.A. Tick, U.S. Patent 437907005 (1983).
28. G.H. Beall and C.J. Quinn, U.S. Patent 507179510 (1991).
29. G.H. Beall and J.E. Pierson, U.S. Patent 5328874 (1994).
30. ISO 5 660-1, *Reaction-to-Fire Tests-Heat Release, Smoke Production and Mass Loss Rate-Part 1 Heat Release Rate (Cone Calorimeter Method)*, 2nd ed., International Standards Organization, Geneva, Switzerland, (2002).
31. K. Weisskopf and G. Meyerhoff, *Polymer*, **24**, 72 (1983).
32. B. Schartel and T.R. Hull, *Fire Mater.*, **31**, 327 (2007).
33. V. Babrauskas and R.D. Peacock, *Fire Saf. J.*, **18**, 255 (1992).
34. J.W. Gilman, C.L. Jackson, A.B. Morgan, R. Harris, E. Manias, E.P. Giannelis, M. Wuthenow, D. Hilton, and S.H. Phillips, *Chem. Mater.*, **12**, 1866 (2000).
35. J. Zhu, F.M. Uhl, A.B. Morgan, and C.A. Wilkie, *Chem. Mater.*, **13**, 4649 (2001).
36. S.V. Levchik, G.F. Levchik, G. Camino, L. Costa, and A.I. Lesnikovich, *Fire Mater.*, **20**, 183 (1996).
37. S.V. Levchik, G. Camino, L. Costa, and G.F. Levchik, *Fire Mater.*, **19**, 1 (1995).
38. S.V. Levchik, L. Costa, and G. Camino, *Polym. Degrad. Stab.*, **36**, 229 (1992).

 DOI 10.1002/pen